Miscibility and Specific Interactions in Blends of Poly(L-Lactide) with Poly(Vinylphenol)

Emilio Meaurio,[†] Ester Zuza,[‡] and Jose-Ramon Sarasua*[,‡]

Departamento de Ingeniería Química y del Medio Ambiente, and Departamento de Ingeniería Minera y Metalúrgica y Ciencia de los Materiales, Escuela Superior de Ingenieros. Universidad del País Vasco, Alameda de Urquijo SN, 48013, Bilbao, Spain

Received October 21, 2004; Revised Manuscript Received December 9, 2004

ABSTRACT: This paper reports a DSC and FTIR study of blends of poly(L-lactide) (PLLA) with poly(vinylphenol) (PVPh). According to the single T_g criterion, miscibility has been found in all the compositions range for the blends obtained by solution/precipitation in a dioxane/hexane pair. However, phase separation has been observed for PVPh-rich blends obtained by solvent casting from dioxane solutions. The T_g of the blends shows negative deviation from linearity. Hydrogen bonding has been found, and the band attributed to hydrogen-bonded carbonyl groups is shifted about 18 cm^{-1}, suggesting relatively weak hydroxyl−ester hydrogen bonds. The equilibrium melting points of pure PLLA and different blends have been recorded, and the values of the interaction parameter $\chi_{12} = -0.42$ and the interaction energy density $B = -8.8$ cal/cm^3 have been calculated. The negative value of the interaction parameter confirms a thermodynamically miscible blend. The value of B is similar to the value found in poly(ϵ-caprolactone) (PCL)/PVPh. This small difference between both systems is feasible because the weaker attractive interactions found in PLLA/PVPh counteract against weaker repulsive interactions, as the solubility parameter of PLLA ($\delta = 10.1$ (cal/cm^3)$^{1/2}$) is closer to PVPh ($\delta = 10.6$ (cal/cm^3)$^{1/2}$) than the solubility parameter of PCL ($\delta = 9.2$ (cal/cm^3)$^{1/2}$).

Introduction

Poly(L-lactide) (PLLA) is well known in the medical industry as a biocompatible and biodegradable polymer for applications such as drug delivery systems,[1] implant materials for bone fixation,[2] and surgical suture.[3] These products slowly hydrolyze within the body to lactic acid in the presence of body fluids. However, the prohibitive cost of producing pure L-lactide isomer via organic chemistry synthesis procedures has restricted their applicability outside this field until the late 1980s. Advances in the bacterial fermentation of glucose obtained from corn introduced the potential to obtain L-lactide considerably cheaper.[4] Moreover, problems associated with the incineration of waste have led to the need for the development of truly biodegradable polymers to be utilized as substitutes for non-biodegradable petrochemical-based polymers in packaging, consumer goods, etc. The good gas barrier properties of PLLA, comparable to PVC and PET, associated to its biodegradability properties, open the possibility of using it as a potential commodity material in the packaging industry. Thus, the study of lactic acid-based polymers is receiving much attention, and presently several companies have announced development activities for polylactides.[4]

However, PLLA has been reported to have poor processing properties and is brittle at room temperature[5]. Several modifications have been proposed to improve processing and mechanical properties, such as copolymerization, plasticization, and polymer blending. Miscibility has been studied with many other polymers, but only a few counterparts have been reported to give miscible blends: poly(DL-lactide) (PDLLA),[6−10] poly(D-lactide) (PDLA),[11−14] poly(3-hydroxybutyrate) (PHB),[15,16] poly(methyl methacrylate) (PMMA),[17,18] poly(methyl acrylate) (PMA),[17] poly(vinyl acetate) (PVAc),[19−22] and poly(ethylene oxide) (POE).[23−26] On the other hand, immiscibility has been found in blends of PLLA with poly(butadiene-*co*-acrylonitrile) (NBR),[27] poly(*p*-dioxanone),[28] poly(3-hydroxybutyrate-*co*-3-hydroxyvalerate) (PHBV),[29] poly(vinyl alcohol) (PVA),[30,31] and poly(4-vinylphenol) (PVPh).[32] Taking into account this global context, the miscibility behavior of PLLA shows a striking difference compared with polyesters of similar nature such as PHB or PCL; PLLA presents an apparently normal variety of miscible counterparts if relatively weak interactions are involved (i.e., mixed with polyesters or polyeters), but unexpected immiscibility results have been found when mixed with polymers capable of strong interactions such as hydrogen bonds (i.e., PVA or PVPh).

Nevertheless, hydrogen bonding is an important mechanism to expand the range of miscible polymer pairs since if no favorable interactions are present miscibility is very rare and is only found when miscibility parameters match each other;[33] if favorable weak interactions are present, miscibility can be found even if the difference in solubility parameters goes up to $\Delta\delta_{crit} = 0.5$ (cal cm^{-3})$^{1/2}$, but when hydrogen bonds are established, it can go up to 3.0 (cal cm^{-3})$^{1/2}$. The present work focuses on the study of miscible blends of PLLA with PVPh, a presumable hydrogen-bonding counterpart, according to the chemical structures shown in Figure 1. This system has been earlier reported to show only partial miscibility,[32] and no specific interactions were observed by FTIR.[34] We have carried out an extensive study of blend preparation conditions and have found complete miscibility if blends are obtained in proper conditions. Interactions have been analyzed by FTIR, and the polymer−polymer intercation parameter has been calculated according to the melting point depression method.

* Author to whom correspondence should be addressed.
[†] Departamento de Ingeniería Química y del Medio Ambiente.
[‡] Departamento de Ingeniería y Metalúrgica y Ciencia de los Materiales.

10.1021/ma047818f CCC: $30.25
Published on Web 01/27/2005

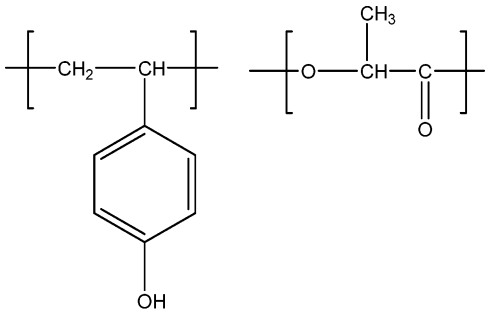

PVPh **PLLA**

Figure 1. Chemical structures of PVPh and PLLA.

Experimental Section

A. Starting Materials. Optically pure poly(L-lactide) containing less than 0.01% of residual solvent and less than 0.1% residual monomer was supplied by PURAC BIOCHEM (Netherlands). Its specific rotation in chloroform at 20 °C was −157.3°. The molecular weight of poly(L-lactide) was measured viscometrically in a Ubbelohde-type viscometer in chloroform at 30 °C, using the relation:[63]

$$[\eta] = 5.45 \times 10^{-4} M_v^{0.73} \text{ (dL/g)} \quad (1)$$

A value of $M_v = 3.2 \times 10^5$ g/mol was obtained.

PVPh was synthesized in our laboratory. This polymer is not usually polymerized from its monomer, vinylphenol, because its free-radical polymerization lacks control over the molecular weight of the polymer because of chain transfer to the phenolic hydrogen.[35] Thus, the PVPh was synthesized by polymerization of acetoxystyrene and subsequent hydrolysis of the acetoxy groups.[36] The monomer was obtained from Sigma, and polymerization was carried out in toluene at 70 °C using benzoyl peroxide (2 mol%) as initiator. The product was precipitated into methanol. The protecting acetoxy groups were removed via hydrazinolisys in tetrahydrofuran at room temperature for 6 h with a 50% excess of hydrazine hydrate. After the reaction was complete, the product was precipitated into water and thoroughly washed. The PVPh was characterized by Fourier transform infrared spectroscopy (FTIR) and differential scanning calorimetry (DSC). The molecular weight of PVPh was measured viscometrically in a Ubbelohde-type viscometer in dioxane at 25 °C, using the relation:[37]

$$[\eta] = 2.03 \times 10^{-4} M_v^{0.66} \text{ (dL/g)} \quad (2)$$

A value $M_v = 3.0 \times 10^4$ g/mol was obtained.

B. Blend Preparation. PLLA and PVPh dissolve in dioxane at temperatures of about 70 °C, and their solutions remain stable at room temperature. Dioxane solutions of the polymers (2 wt%) were mixed in the desired amounts. Blends were prepared by solvent casting at 30 °C or by precipitation in a large excess of *n*-hexane and then were dried in a vacuum oven at 50 °C for 2 days.

C. Differential Scaning Calorymetry. Thermal analysis was carried out on a DSC from TA Instruments, model DSC 2920. Approximately 5−10 mg of each blend was weighted and sealed in an aluminum pan. Two consecutive scans were performed, with a scan rate of 20 °C/min, up to 200 °C to ensure complete melting of the sample. Glass transition temperatures were obtained in the second scan and were measured as middle point values. For melting point depression studies, samples were allowed to crystalize isothermally until crystallization was complete and were then heated with a scan rate of 10 °C/min to obtain the melting point values.

D. Infrared Spectroscopy. Infrared spectra of blends were recorded on a Nicolet AVATAR 370 Fourier transform infrared spectrophotometer. Spectra were taken with a resolution of 2 cm^{-1} and were averaged over 64 scans. Dioxane solutions containing the blends were cast on KBr pellets, and samples were vacuum-dried at 60 °C for 48 h. In the case of the blends obtained by precipitation, a small quantity of the sample was mixed with KBr, carefully ground in a mill, dried at 110 °C for an hour to remove moisture, and pressed in a hot mold. The absorbance of all the studied samples was within the absorbance range in which the Lambert−Beer law is obeyed. Second derivative spectra were smoothed with a quartic 15-point Savitzky-Golay smoothing filter.[38] Corrected coefficients are found in reference 39. Following the Edwards et al.[40] suggestions, the degree of distortion of this smoothing algorithm was checked by the following procedure. A synthetic spectrum of similar shape to these to be smoothed was generated, and its second derivative was calculated with the smoothing coefficients. The unsmoothed second derivative of the synthetic spectrum was also calculated. Both spectra were visually inspected. Only very subtle changes were observed with this smoothing algorithm. Thus, the degree of distortion introduced by smoothing should be considered negligible.

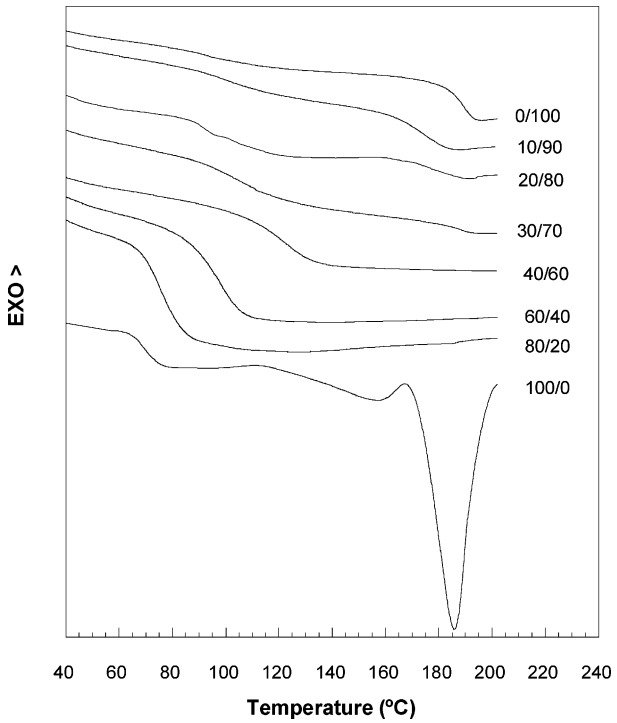

Figure 2. Second scan DSC traces for PLLA, PVPh, and PLLA/PVPh blends of different compositions obtained by solvent casting.

Results and Discussion

DSC Analysis. Miscible polymer pairs show a single glass transition temperature (T_g) intermediate between those of the pure polymers which makes DSC a well-known method to study the miscibility of polymer blends. Blends were obtained by solvent casting from dioxane solutions and by solution/precipitation in a dioxane/hexane pair, leading to somewhat different results, as is discussed later on.

The DSC traces of pure PLLA and PVPh are shown in Figure 2. PLLA is a semicrystalline polymer, and the major features of its DSC curve are the T_g at ∼70 °C, and its melting peak at 187 °C. PVPh is an amorphous polymer, and the T_g of the sample used in this work is 190 °C. In blends cast from dioxane solutions, two successive scans were recorded from 0−200 °C. Figure 2 also shows DSC traces obtained in the second scan for PLLA/PVPh blends with different compositions. As can be seen, a single T_g is obtained for compositions between pure PLLA and the PLLA/PVPh 40:60 blend.

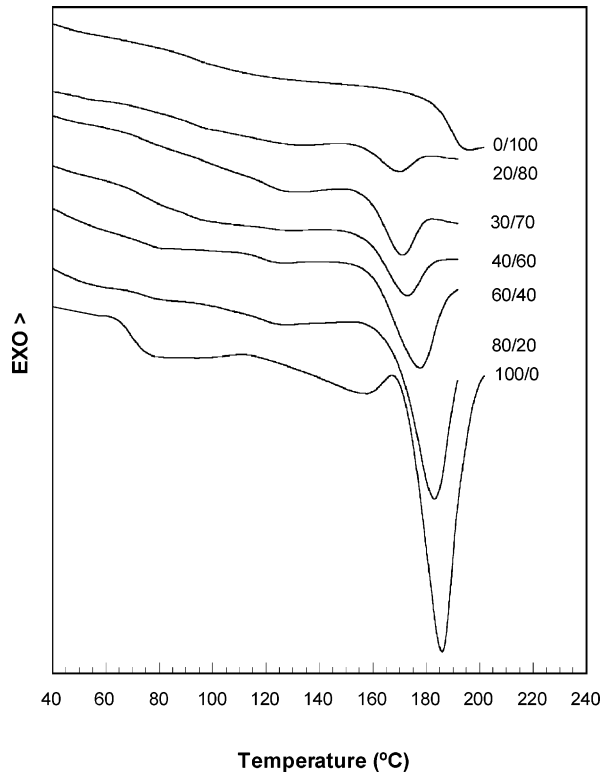

Figure 3. First scan DSC traces for PLLA, PVPh, and PLLA/PVPh blends of different compositions obtained by solution/precipitation.

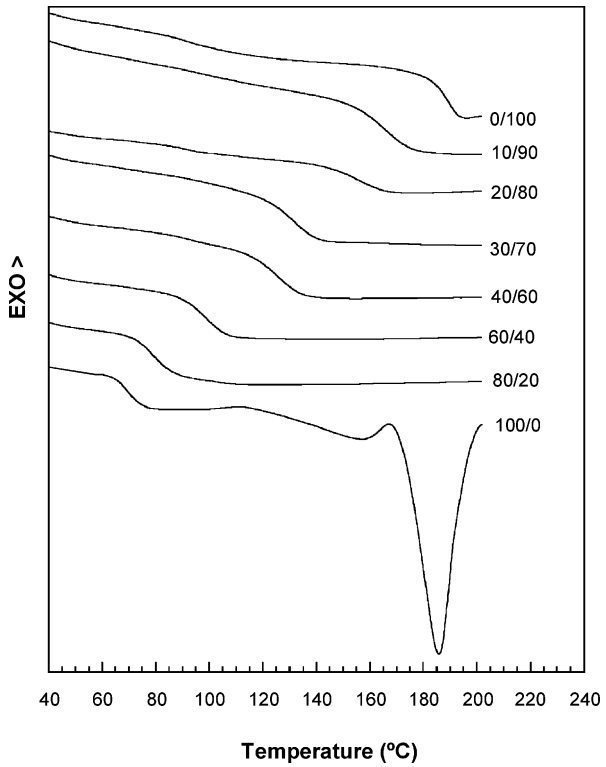

Figure 4. Second scan DSC traces for PLLA, PVPh, and PLLA/PVPh blends of different compositions obtained by solution/precipitation.

However, blends with compositions ranging from PLLA/PVPh 30:70 to pure PVPh show two T_g's; one of the transitions is very broad and is placed at a temperature close to the T_g of the single-phase PLLA/PVPh 60:40 blend, and the second T_g is close to that of pure PVPh. Thus, for the molecular weights employed in this study, a single phase is obtained if the content of PVPh in the blend is below 60 wt%. However, in blends exceeding 60 wt% PVPh, the system undergoes phase separation, giving one phase with a composition close to 60:40 and a second phase consisting mainly of PVPh.

Figure 3 shows DSC traces recorded in the first scan for PLLA/PVPh blends of different composition, obtained by solution/precipitation in the dioxane/hexane pair. All the scans show a melting peak corresponding to crystalline PLLA. Nevertheless, systems rich in PLLA show a broad specific heat jump at temperatures close to the glass transition of pure PLLA. This situation suggests phase-separated systems, although a second specific heat jump attributable to the PVPh-rich phase cannot be observed because of the strong endotherm due to melting of PLLA crystals. These curves are also very similar to those obtained in the first scan for solution-cast blends.

However, DSC traces change completely in the second scan taken after cooling from the melt to room temperature for the solution/precipitation blends. As can be seen in Figure 4, a single T_g is obtained in all the composition range, proving the miscibility of the blends. In addition, the strong melting endotherm of PLLA disappears for the whole blend composition range. These results can be explained in the following terms. In the solution/precipitation blends, polymer chains are "frozen" in the precipitation step, and if specific interactions between different chains in the solution are neglected, a random dispersion of chains can be assumed in the precipitated blends. After the first heating scan, the sample is completely melted, the system history is erased, and the blends become miscible. On the other hand, in the solution-cast blends, different phase domains can develop as the solvent evaporates due to favorable solvent−polymer interactions that tend to exclude the second component from the growing domains. Phase separation is then induced by the solvent, a phenomenon known as $\Delta\chi$ effect.[41,42] Thus, the system is phase separated in macroscopic domains, and a heating run up to total melting of the sample cannot restore the thermodynamic equilibrium conditions. A similar behavior has been reported by Zhang et al.[18] in blends of PLLA with PMMA; they also found phase separation in solution-cast blends and miscibility in blends obtained by solution/precipitation.

In addition, when the melt is rapidly lowered to an isothermal temperature of 148 °C and is maintained there for 1 h (Figure 5), just PLLA-rich compositions are able to crystallize while PLLA/PVPh blends containing higher than 30 wt% PVPh remain amorphous. This behavior is typical of miscible blends in which the second component mixes at a molecular level inhibiting crystallization of the crystalline component.

The dependence of T_g on the composition of the miscible PLLA/PVPh blends is illustrated in Figure 6 (see Table 1 for numerical values). Several equations have been proposed to describe the T_g−composition dependence of miscible polymer blends. Couchman and Karasz[43] proposed a general equation for predicting the T_g of polymer blends, based on the continuity of the entropy of mixing at T_g, from which the most classical models, such as the Fox or Gordon-Taylor can be derived. Although these equations have been successfully applied to certain blends, there are still systems with significant deviations; particularly severe devia-

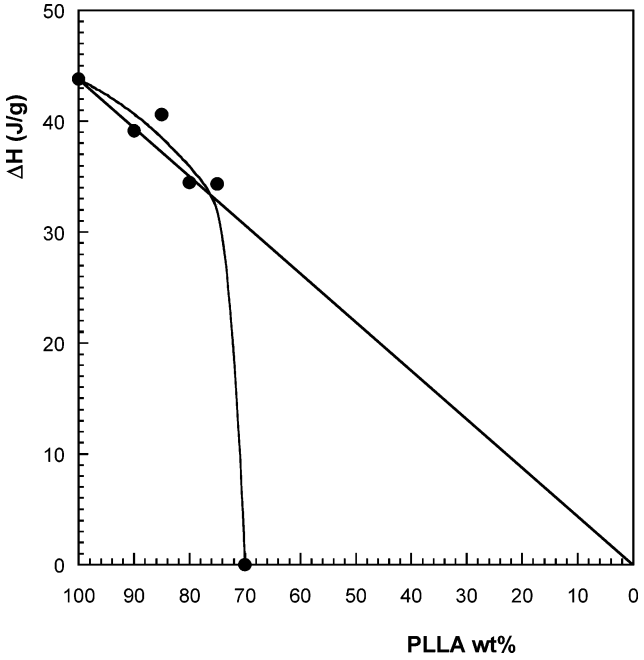

Figure 5. Enthalpy of fusion versus composition for PLLA/PVPh blends annealed at 148 °C for 1 h.

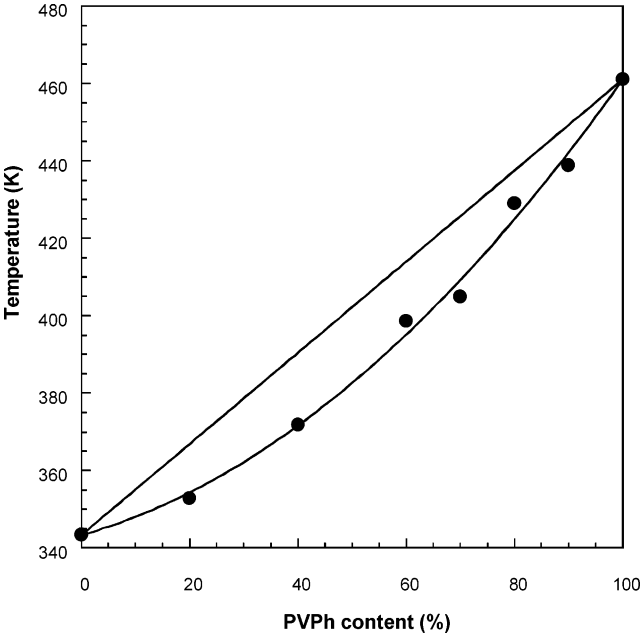

Figure 6. T_g vs composition for PLLA/PVPh blends. The straight line represents linear behavior, and the curve is the fit to the simplified Kwei equation ($q = -78$).

tions are shown by systems containing hydrogen bonding. In these cases, the most suitable relationship is the Kwei equation:[44]

$$T_g = \frac{w_1 T_{g1} + k w_2 T_{g2}}{w_1 + k w_2} + q w_1 w_2 \quad (3)$$

where w_1 and w_2 are the weight fractions of components 1 and 2, respecively, T_{g1} and T_{g2} are the glass transitions, and k and q are fitting constants. The first term on the right-hand side of eq 3 is the widely used Gordon-Taylor equation, and the second term corresponds to the strength of hydrogen bonding in the blend, reflecting a balance between the breaking of the self-association

Table 1. T_g Values for PLLA/PVPh Blends of Different Composition

PVPh wt%	T_g (°C)	PVPh wt%	T_g (°C)
0	70.2	70	131.7
20	79.6	80	155.8
40	98.6	90	165.7
60	125.4	100	187.9

interactions and the forming of the interassociation interactions through hydrogen bonding. In systems with a highly symmetric deviation from linearity, it is common practice to set $k = 1$; fitting to a single parameter, with a simplified Kwei equation:

$$T_g = w_1 T_{g1} + w_2 T_{g2} + q w_1 w_2 \quad (4)$$

The fit of experimental data to the Kwei equation is also shown in Figure 6, and the value obtained for the adjustable parameter is $q = -78$. This large negative value for q suggests that the specific interactions responsible for miscibility are weak.

FTIR Analysis. Infrared spectroscopy has been widely used to investigate specific interactions in polymer blends in which the miscibility driving force is hydrogen bonding between components. The distribution of the different association species is dependent upon the composition of the mixture, the temperature, and the equilibrium constants describing both self- and interassociation.

The chemical structures of the studied polymers support the possibility of hydrogen bonding between hydroxyl groups of PVPh and carbonyl groups of PLLA. Miscibility between PVPh and polyesters of similar nature of PLLA, such as poly(hydroxybutirate)[45] and poly(ϵ-caprolactone) (PCL),[46] has also been reported, and hydrogen bonding has been confirmed by FTIR in these systems. However, Zhang et al. studied blends of PVPh with polylactides and did not find evidence of specific interactions by FTIR.[34] Only partial miscibility was obtained, according to their study. Our results support total miscibility and existence of specific interactions, although these are weaker than in other PVPh/polyester systems.

Recording of FTIR spectra and sample preparation have not been straightforward tasks. DSC results have shown that it is necessary to melt PLLA to achieve miscibility; thus, all spectra were recorded in the cooling step after melting at 200 °C for 2 min. FTIR samples with up to 60 wt% PVPh were obtained by solvent casting on KBr pellets because DSC results showed a single T_g for those compositions. Since the solvent casting method resulted in phase separation with PVPh amounts higher than 60 wt%, FTIR samples with 80% and 90% PVPh were obtained by mixing the blend obtained by solution/precipitation with KBr in a mill, grinding carefully, and pressing in a mold at 110 °C to remove moisture. An appropriate spectra for the blend with 70% PVPh could not be obtained by the grinding method.

The chemical groups involved in hydrogen bonding of this polymer blend system are the hydroxyl of PVPh and carbonyl of PLLA, and their absorption band regions are of major concern to study their eventual interassociation behavior. Figure 7 shows the hydroxyl spectral region of pure PVPh and PLLA/PVPh blends of different composition. PVPh shows two contributions attributable to the free and associated hydroxyl groups, respectively. The broad band governing this region is

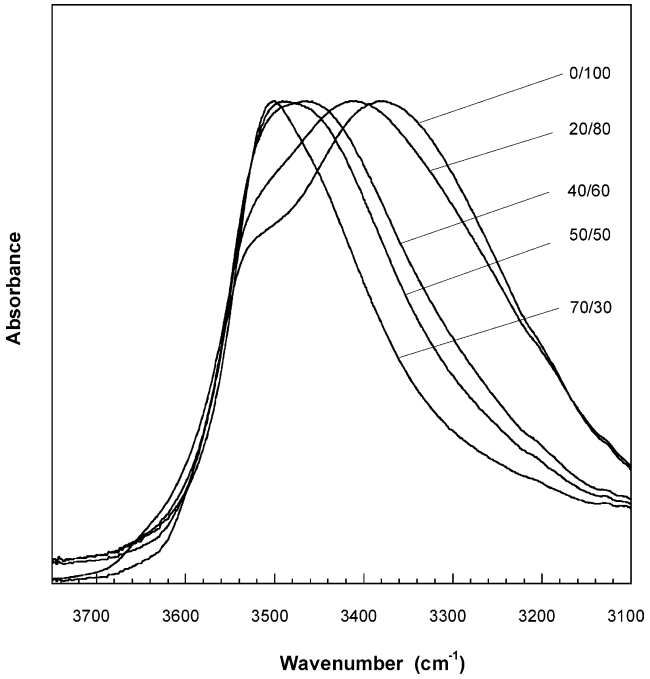

Figure 7. Hydroxyl stretching region for PLLA/PVPh blends of different composition at room temperature.

centered at about 3360 cm^{-1} and corresponds to the associated hydroxyl contribution. The free hydroxyl band appears as a relatively narrow shoulder at about 3525 cm^{-1}. Analyzing PLLA/PVPh spectra, it can be observed that the relative contribution of the hydrogen-bonded hydroxyl group increases as the concentration of PLLA in the blend increases; in addition, the hydrogen-bonded hydroxyl band shifts to higher frequencies. The change in relative intensities is attributed to a higher overall extent of interassociation that lowers the fraction of free hydroxyl groups. The shift of the associated hydroxyl band to higher frequencies is attributed to the replacement of the hydroxyl stretching band of hydroxyl−hydroxyl hydrogen-bonded groups existing in pure PVPh by a new band in blends corresponding to hydroxyl groups of PVPh bonded to carbonyl groups of PLLA. The frequency shift between the free hydroxyl and the hydrogen-bonded hydroxyl band is related to the strength of the bond and varies at 25 °C from about 165 cm^{-1} in pure PVPh to about 25 cm^{-1} in a PLLA/PVPh 70:30 system. This low shift value indicates that the hydroxyl−ester interactions are weaker than hydroxyl−hydroxyl interactions existing in pure PVPh.

Figure 8a shows the carbonyl stretching region of PLLA at different temperatures. In Figure 8b and c, second derivatives and spectral curve fitting results for amorphous and semicrystalline PLLA are displayed. The spectrum of pure PLLA at temperatures above the melting point exhibits a broad and asymmetric peak (Figure 8b). The second derivative of this spectrum reveals clearly two components; spectral fitting with two Gaussian peaks gives a good fit at locations 1755 and 1776 cm^{-1}. Amorphous PLLA has been earlier analyzed by Kister at al.,[47,48] who reported broad and asymmetric bands in the Raman spectra in which the deconvolution analysis showed two components centered at 1749 and 1768 cm^{-1}. The splitting of the carbonyl band was attributed to the sensitivity of the C=O stretching mode to conformation, and the double bands were considered as resulting from the particular chiral unit enchainments generated by the pair addition mechanism which governs the LA ring opening polymerization.[48] The IR components at 1755 and 1776 cm^{-1} obtained in this work can be assigned to the corresponding Raman components at 1749 and 1768 cm^{-1}. On the other hand, below the melting point, an additional component is expected due to absorption of the crystalline morphology. As can be seen in Figure 8a, raising the temperature from 100 to 180 °C lowers the absorbance at the center of the peak, and simultaneously the intensity of a shoulder at lower wavenumbers increases. Spectral fitting of this region (Figure 8c) reveals three contributions at 1757, 1759, and 1777 cm^{-1}. The components at 1757 and 1777 cm^{-1} are assigned to the amorphous phase. The narrow band at 1759 cm^{-1} is attributed to the crystalline absorption and is visually discerned from the broad absorption at 1757 cm^{-1} due to the marked

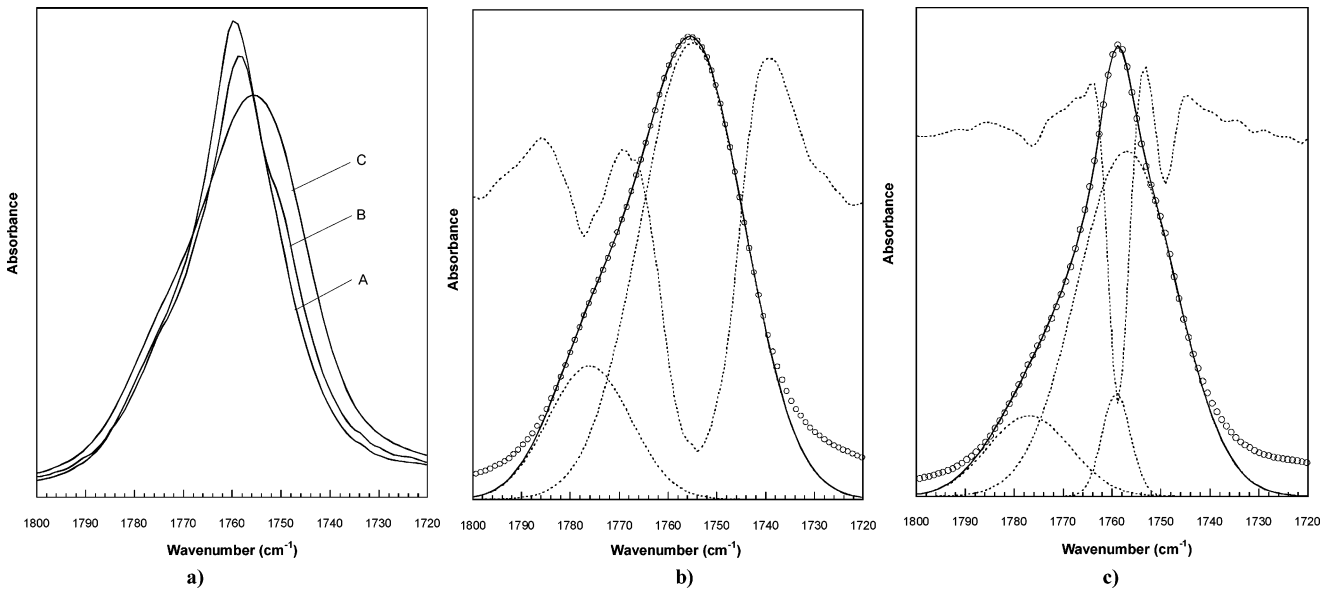

Figure 8. (a) Carbonyl stretching region of PLLA at different temperatures: (A) at 100 °C in the heating process, (B) at 180 °C in the heating process, and (C) at 160 °C in the cooling process after melting (amorphous PLLA). (b) Second derivative spectra and the curve fitting components obtained for amorphous PLLA at 160 °C. (c) Second derivative spectra and the curve fitting components obtained for semicristalline PLLA at 100 °C. Heating and cooling processes were carried out at 5 °C/min.

Table 2. Spectral Curve Fitting Results for Amorphous and Semicrystalline PLLA[a]

	Peak 1			Peak 2			Peak 3		
	ν (cm^{-1})	W (cm^{-1})	area (%)	ν (cm^{-1})	W (cm^{-1})	area (%)	ν (cm^{-1})	W (cm^{-1})	area (%)
amorphous PLLA (160 °C)	1776.1	20	18.8	1755.0	24	81.2	-	-	-
semicrystalline PLLA (100 °C)	1777.0	20	15.2	1757.0	24	78.1	1759.1	6.85	6.7

[a] Peak 1 and 2 refer to the two amorphous absorptions, and Peak 3 refers to the crystalline component.

difference in widths. Numerical results are summarized in Table 2.

As a final comment in Figure 8c, the second derivative spectra displayed may seem somewhat uncorrelated to the curve fitting results. For example, the intensity obtained from curve fitting results for the crystalline absorption is relatively weak, but this band is by far the sharpest contribution in the second derivative spectra. Derivation increases spectral resolution, but when it is performed on overlapping bands with different widths, it also results in the increase of the relative intensity of the narrower band. This can be easily proved by deriving twice the mathematical equation for a Gaussian profile and calculating the intensity ratio at the maximum for two hypothetical overlapping peaks (1 and 2):

$$\frac{(A_0)_1}{(A_0)_2} = \frac{(A_0)_1}{(A_0)_2}\left(\frac{w_2}{w_1}\right)^2 \qquad (5)$$

where subscripts 1 and 2 refer to the different bands 1 and 2; A_0 is the intensity of the second derivative peak, A_0 is the absorbance of the spectral component at the maximum, and w is the width of the band. Another consequence of this derivative behavior on results displayed in Figure 7c is that spectral derivation suggests an amorphous component located at about 1749 cm^{-1}, but curve fitting locates this band at 1757 cm^{-1}. This discrepancy is due to the intense side lobe of the crystalline peak in the second derivative that sinks the second derivative contribution corresponding to the amorphous band. It can be easily proved that the obtained second derivative spectrum is compatible with the curve fitting results by generating a synthetic spectrum of similar shape (see Table 2) and obtaining its second derivative. Thus, second derivative techniques are valuable to analyze the number of components, but peak positions should be taken with care, particularly in the case of highly overlapping peaks of very different widths.

Figure 9 shows the carbonyl stretching region for PLLA/PVPh obtained after cooling from the melt at 30 °C. It has to be noted that PLLA/PVPh blends studied in this figure are fully amorphous, as confirmed by DSC in Figure 5. Therefore, no crystalline absorption is expected in these spectra. The band obtained for PLLA at 160 °C in the cooling process (amorphous) is shown for reference. As can be observed in Figure 9, the carbonyl band becomes wider as the PVPh content in the blend increases. This behavior is attributed the presence of a new band at about 1740 cm^{-1}, assigned to the hydrogen-bonded carbonyl groups, indicative of the intermolecular interaction involving the PLLA carbonyl group and the PVPh hydroxyl group. However, the low resolution in this spectral region may let some doubts about the qualitative trends in this region remain. For example, the relative contribution attributed to the associated carbonyl seems to get stuck for compositions higher than 60 wt% PVPh. Another question relates the number of bands present in this region. To clarify these questions, second derivative spectra are shown in Figure 10. The main advantage of spectral derivation is to increase the resolution of the

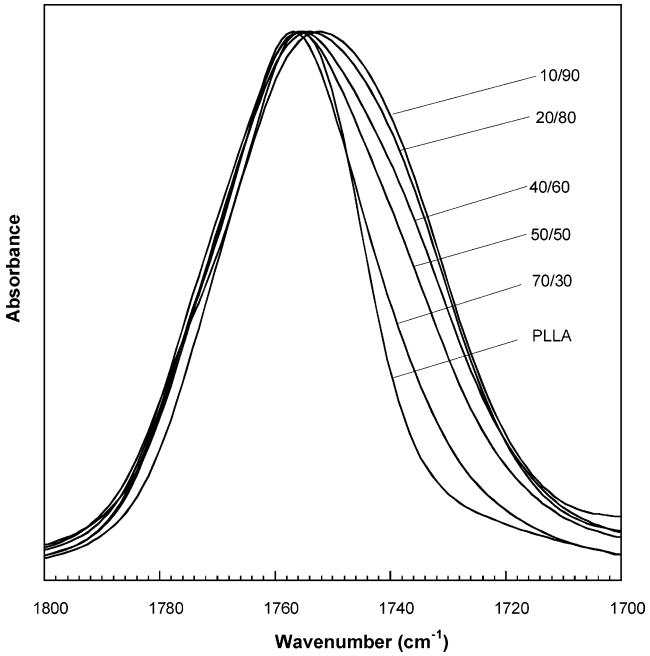

Figure 9. Carbonyl stretching region for amorphous PLLA (at 160 °C) and PLLA/PVPh blends of different composition at room temperature.

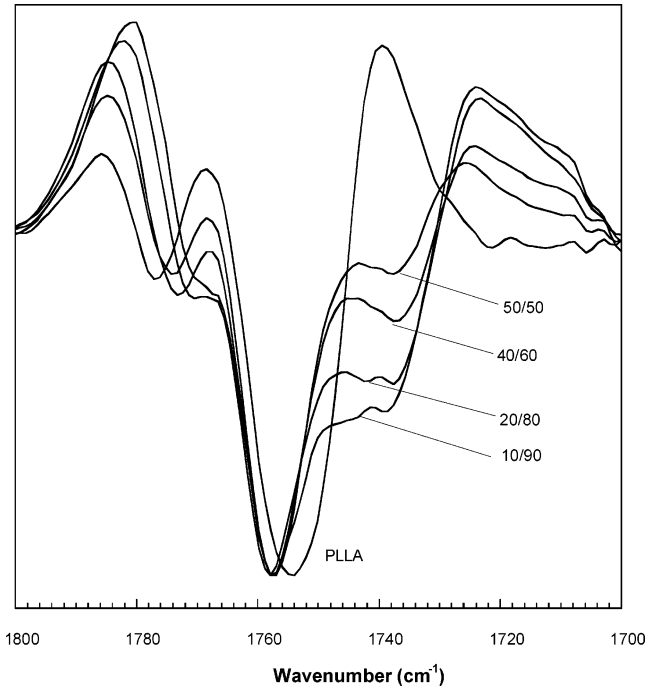

Figure 10. Second derivative of the carbonyl stretching region for amorphous PLLA (at 160 °C) and fully amorphous PLLA/PVPh blends of different composition at room temperature.

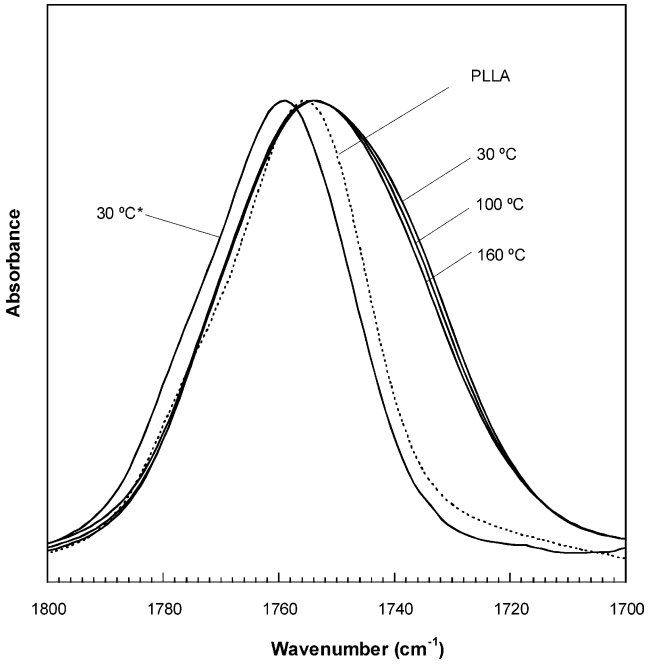

Figure 11. Temperature dependence of the carbonyl spectral region for a PLLA/PVPh 20:80 blend taken on cooling from the melt at 160, 100, and 30 °C. The spectrum marked with an asterisk was obtained from the as-precipitated blend at 30 °C before melting. The spectrum of PLLA at 160 °C is also shown for reference.

spectra. Another feature is that the contribution of any linear baseline is eliminated. Figure 10 suggests that the relative absorption of the hydrogen-bonded band at about 1740 cm^{-1} increases steadily as the content of PVPh increases. This is true if the widths of the components remain approximately constant between different compositions, which seems to be a reasonable assumption. Also, second derivative spectra show the presence of three components for all the compositions corresponding to the above-mentioned hydrogen-bonded band and the two original bands assigned to amorphous PLLA.

The temperature dependence of the interassociation behavior has also been studied. Figure 11 shows the spectra of a PLLA/PVPH 20:80 blend prior to any heating process. This specific band was obtained from a sample dried at low temperatures to avoid crystallization of PLLA. The carbonyl band is broad, typical of the amorphous phase, and no interassociation shoulder is observed. The absence of interassociation in the as-obtained sample agrees with the phase separation obtained in the first heating scans by DSC. This figure also shows the scale-expanded spectra of a PLLA/PVPh 20:80 blend obtained from a different pellet that was carefully dried to obtain appropriate spectra on cooling from the melt at 160, 100, and 30 °C. It can be observed that a clear shift to lower wavenumbers in these spectra taken on cooling with respect to the as obtained 30 °C spectrum occurs, which indicates that interassociation via hydrogen bonding has taken place in this miscible blend. It is also observed that the change of the band shape among spectra taken at different temperatures is very small and suggests that the associated band shifts to higher wavenumbers and/or its relative intensity decreases at higher temperatures. Shifting to higher wavenumbers is attributed to weaker hydrogen bonds at higher temperatures, and the decrease in intensity is mainly related to the interchange between free and hydrogen-bonded carbonyls, although some contribution can be explained by the decrease of the molar extinction coefficient of the hydrogen-bonded band.[64]

Finally, we find it necessary to briefly discuss the possible reasons of the splitting observed for the carbonyl band of molten PLLA. This is an unusual behavior because typical polyesters with chemical structure similar to that of PLLA show a single band in the carbonyl spectral region in the amorphous conformation.[45−57] The only reference reporting this behavior for poly(lactides) attributes splitting of the carbonyl band to the sensitivity of the C=O stretching mode to conformation.[47,48] However, this explanation lacks of a theoretical background and is rather arguable for an amorphous polymer. Splitting has also been found in low-molecular-weight species. For example, FTIR spectra for a series of solid esters and ketones[50,51] showed splittings of about 10 cm^{-1}, attributed to the isolation of molecules within multiple types of matrix sites. The presence of such different sites is, however, questionable. Splitting has also been found in the carbonyl spectral region of organic liquids; for example, cyclohexanone shows a splitting of 16 cm^{-1},[52] attributed to Fermi resonance.[53] This type of splitting is accepted to occur often with carbonyl vibrations in complex organic molecules, although in the majority of cases, the frequency match of the overtone and fundamental is relatively poor.[54] However, experimental evidences show that the description of the splitting of cyclohexanone from a Fermi resonance approach is inconsistent.[53,55] Recently, the splitting of cyclohexanone has been revised and strong experimental evidence of C−H···O hydrogen bonding has been reported.[52,65] Evidences of this type of hydrogen bonding have also been reported in matrix-isolated low-molecular-weight compounds[49] and in neat polymers.[56] This global context reveals that today the assignment of this type of carbonyl splitting is under discussion.

Equilibrium Melting Temperature: Melting Point Depression. The depression of the melting point of a crystalline polymer blended with an amorphous polymer can be studied to obtain information about the miscibility of the system. The temperature reduction is caused by morphological effects and thermodynamic reasons. Thermodynamic considerations predict that the chemical potential of a polymer will be decreased by the addition of a miscible diluent. If the polymer is crystallizable, this decrease in chemical potential will result in a decreased equilibrium melting point. The equilibrium melting temperatures can be analyzed by the Flory−Huggins equation:[58]

$$\frac{1}{T_m^{\,0}} - \frac{1}{T_{mb}^{\,0}} = \frac{-R}{\Delta H_{2u}} \frac{V_{2u}}{V_{1u}} \left[\frac{\ln \phi_2}{x_2} + \left(\frac{1}{x_2} - \frac{1}{x_1} \right) (1 - \phi_2) + \chi_{12} (1 - \phi_2)^2 \right] \quad (6)$$

where the subscripts 1 and 2 refer to the amorphous and the crystallizable polymer, respectively. $T_m^{\,0}$ and $T_{mb}^{\,0}$ denote the equilibrium melting points of the pure crystallizable component and of the blend, respectively. V_u is the molar volumes of the repeating unit of the polymers, R is the universal gas constant, ΔH_u is the heat of fusion of the perfectly crystallizable polymer, x is the degree of polymerization, ϕ is the volume fraction of the component in the blend, and χ_{12} is the polymer−

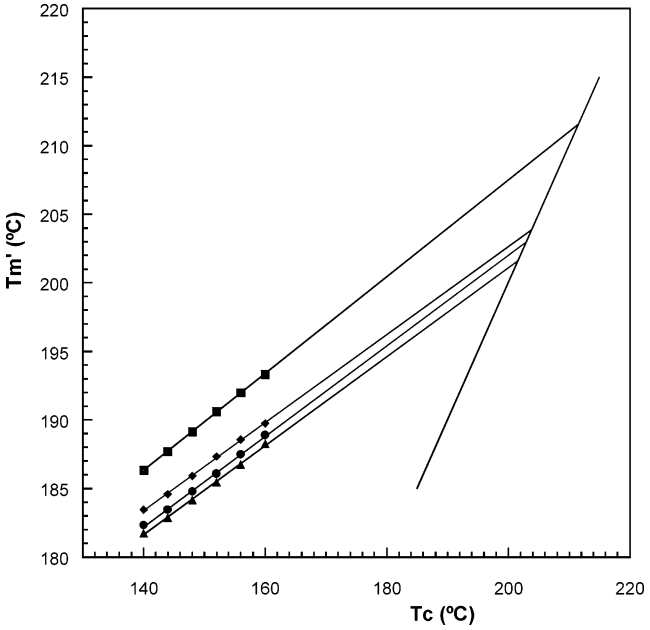

Figure 12. Hoffman–Weeks plots for PLLA/PVPh blends of different composition: (■) 100:0, (♦) 90:10, (●) 85:15, and (▲) 80:20.

polymer interaction parameter. When both x_1 and x_2 are large, for high-molecular-weight polymers, these related terms can be neglected:

$$-\left(\frac{1}{T_m^0}-\frac{1}{T_{mb}^0}\right)\frac{\Delta H_{2u}}{R}\frac{V_{1u}}{V_{2u}}=\chi_{12}\phi_1^2 \qquad (7)$$

If χ_{12} is assumed to be independent of composition, a plot of the left-hand side of eq 7 versus ϕ_1^2 should give a straight line passing through the origin. The interaction parameter is implicitly referred to a reference volume, V_r, usually defined in terms of the molar volume of the amorphous component in the mixture. This peculiarity makes χ inadequate to compare different systems since the monomer volumes of polymers 1 and 2 are usually significantly different from each other. The interaction energy density is a different form to express the Flory–Huggins interaction parameter eliminating the reference volume:

$$B=\frac{RT\chi_{12}}{V_r} \qquad (8)$$

Substituting χ_{12} from this equation in the Flory–Huggins equation yields the Nishi Wang equation:[59]

$$T_m^0-T_{mb}^0=T_m^0\frac{BV_{2u}}{\Delta H_{2u}}\phi_1^2 \qquad (9)$$

To eliminate the morphological effect from the melting point depression and to determine the equilibrium melting temperatures for pure PLLA and blends of given compositions, the method of Hoffman and Weeks has been used.[60] Values obtained for the equilibrium melting point from the Hoffman–Weeks plot (Figure 12) are summarized in Table 3. The decrease in the equilibrium melting point obtained upon addition of PVPh to pure PLLA suggests the miscibility of the system. However, further addition of PVPh causes a low incremental decrease of the melting point, suggesting a relatively low value for the interaction parameter.

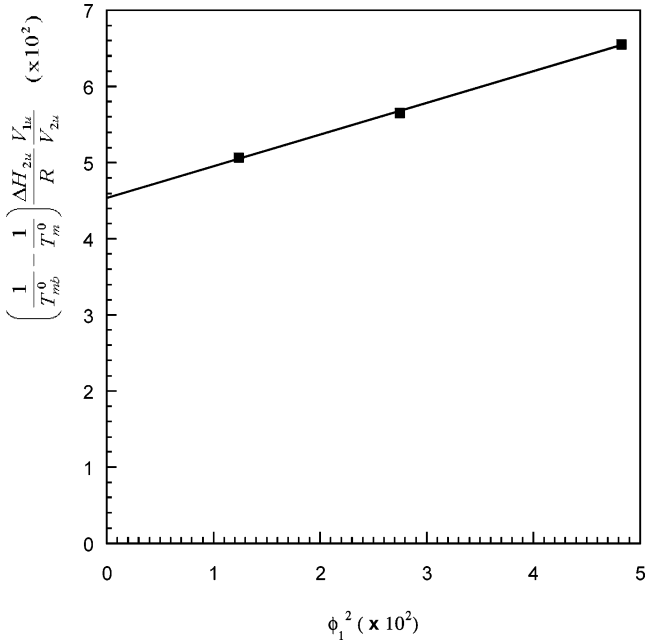

Figure 13. Flory–Huggins equation plot for the equilibrium melting temperatures obtained for PLLA/PVPh blends.

Table 3. Equilibrium Melting Temperature (T_m^0) for Pure PLLA and PLLA/PVPh Blends

PLLA wt%	T_m^0 (°C)
100	211.6
90	203.9
85	203.0
80	201.7

Figure 13 displays the analysis of these values with the Flory–Huggins equation. The parameters used in the calculations are V_{1u} = 100 cm^3, V_{2u} = 53.3 cm^3 (reported earlier in this work), and ΔH_{2u} = 93 J/g.[61] The experimental data fit a line not passing through the origin. This behavior is usually attributed to a residual entropy effect, which is neglected in the derivation of the equation.[62] The values obtained for χ_{12} and B are, respectively, −0.42 and −8.8 J/cm^3. The negative value of the interaction parameter confirms a thermodynamically miscible blend. The value of B is similar to the value found in PCL/PVPh.[46] The analysis of miscibility quantified by interaction parameter proves that both PLLA and PCL systems involve a similar favorable energy exchange with PVPh. This value is the balance between favorable specific interactions and repulsive dispersive interactions. In the case of PCL/PVPh, the specific interactions are stronger than in PCL/PVPh, but this is counterbalanced by more similar solubility parameters existing in PLLA/PVPh with respect to PCL/PVPh.

Conclusions

Miscibility has been found in the PLLA/PVPh system in all the compositions range for blends obtained by solution/precipitation in the dioxane/hexane pair. However, phase separation has been observed for PVPh-rich blends obtained by solvent casting from dioxane solutions. These results have been explained in the following terms. In the solution/precipitation blends, polymer chains are "frozen" in the precipitation step, and if specific interactions between different chains in the

solution are neglected, a random dispersion of chains can be assumed. However, after the first heating scan, the sample is completely melted, the system history is erased, and the blends become miscible. On the other hand, in the solution-cast blends, different phase domains can develop as the solvent evaporates due to favorable solvent−polymer interactions that tend to exclude the second component from the growing domains. Phase separation is then induced by the solvent, a phenomenon known as $\Delta\chi$ effect.

Hydrogen bonding has been found, and the band attributed to hydrogen-bonded carbonyl groups is shifted about 18 cm^{-1}, suggesting relatively weak hydroxyl−ester hydrogen bonds. Finally, the equilibrium melting point of pure PLLA and different blends has been recorded, and the values of the interaction parameter $\chi_{12} = -0.42$ and the interaction energy density $B = -8.8$ cal/cm^3 have been calculated. The negative value of the interaction parameter confirms a thermodynamically miscible blend. The value of B is similar to the value found in PCL/PVPh. This small difference is feasible because the weaker attractive interactions found in PLLA/PVPh counteract against weaker repulsive interactions, as the solubility parameter of PLLA ($\delta = 10.1$ $(cal/cm^3)^{1/2}$) is closer to PVPh ($\delta = 10.6$ $(cal/cm^3)^{1/2}$) than the solubility parameter of PCL ($\delta = 9.2$ $(cal/cm^3)^{1/2}$).

Acknowledgment. The authors are thankful for financial support from MCYT (Project MAT2002-03384) and The University of Basque Country (Project 1/UPV 00151.345-T-15625/2003).

References and Notes

(1) Zhu, K. L.; Xiangzhou, L.; Shilin, Y. *J. Appl. Polym. Sci.* **1990**, *39*, 1.
(2) Bergsma, J. E.; Bos, R. R. M.; Rozema, F. R.; Jong, W. D.; Boering, G. *J. Mater. Sci.: Mater. Med.* **1996**, *7*, 1.
(3) Fambri, L.; Pergoretti, A.; Fenner, R.; Incardona, S. D.; Migliarisi, C. *Polymer* **1997**, *38*, 79.
(4) Lunt, J. *Polym. Degrad. Stab.* **1998**, *59*, 145−152.
(5) Zhang, L.; Goh, S. H.; Lee, S. Y. *Polymer* **1998**, *39*, 4841−4847.
(6) Jorda, R.; Wilkes, G. L. *Polym. Bull.* **1988**, *20*, 479.
(7) Tsuji, H.; Ikada, Y. *Macromolecules* **1992**, *25*, 5719.
(8) Tsuji, H.; Ikada, Y. *J. Appl. Polym. Sci.* **1995**, *58*, 1793.
(9) Tsuji, H.; Ikada, Y. *Polymer* **1996**, *37*, 595.
(10) Tsuji, H.; Ikada, Y. *J. Appl. Polym. Sci.* **1997**, *63*, 855.
(11) Tsuji, H.; Ikada, Y. *Polymer* **1999**, *40*, 6699−6708.
(12) Yamane, H.; Sasai, K. *Polymer* **2003**, *44*, 2569−2575.
(13) Tsuji, H.; Fukui, I. *Polymer* **2003**, *44*, 2891−2896.
(14) Urayama, H.; Kanamori, T.; Fukushima, K.; Kimura, Y. *Polymer* **2003**, *44*, 5635−5641
(15) Blümm, E.; Owen, A. J. *Polymer* **1995**, *36*, 4077.
(16) Focarete, M. L.; Scandola, M.; Dobrzynski, P.; Kowalczuk, M. *Macromolecules* **2002**, *35*, 8472−8477.
(17) Eguiburu, J. L.; Iruin, J. J.; Fernandez-Berridi, M. J.; San Roman, J. *Polymer* **1998**, *39*, 6891−6897.
(18) Zhang, G.; Zhang, J.; Wang, S.; Shen, D. *J. Polym. Sci., Part B: Polym. Phys.* **2003**, *41*, 23−30.
(19) Gajria, A. M.; Dave, V.; Gross, R. A.; McCarthy, S. P. *J. Appl. Polym. Sci.* **1997**, *37*, 437.
(20) Ogata, N.; Jimenez, T. *J. Polym. Sci., Part B: Polym. Phys.* **1997**, *35*, 389.
(21) Yoon, J. S.; Oh, S. H.; Kim, M. N.; Chin, I. J.; Kim, Y. H. *Polymer* **1999**, *40*, 2303−2313.
(22) Park, J. W.; Im, S. S. *Polymer* **2003**, *44*, 4341−4354.
(23) Nakafuku, C.; Sakoda, M. *Polym. J.* **1993**, *25*, 909; **1994**, *26*, 680.
(24) Tsuji, H.; Smith R.; Bonfield W.; Ikada, Y. *J. Appl. Polym. Sci.* **2000**, *75*, 229.
(25) Nakafuku, C. *Polym. J.* **1996**, *28*, 568.
(26) Nijenhuis, A. J.; Colstee, E.; Grijpma, D. W.; Pennings, A. J. *Polymer* **1996**, *37*, 5849−5857.
(27) Park, E. U.; Kim, H. K.; Shim, J. H.; Kim, H. S.; Jang, L. W.; Yoon, J. S. *J. Appl. Polym. Sci.* **2004**, *92*, 3508−3513.
(28) Pezzin, A. P. T.; Alberda van Ekenstein, G. O. R.; Zavaglia, C. A. C.; ten Brinke, G.; Duek, E. A. R. *J. Appl. Polym. Sci.* **2003**, *88*, 2744−2755.
(29) Ferreira, B. M. P.; Zavaglia, C. A. C.; Duek, E. A. R. *J. Appl. Polym. Sci.* **2002**, *86*, 2898−2906.
(30) Tsuji, H.; Muramatsu, H. *J. Appl. Polym. Sci.* **2001**, *81*, 2151−2160.
(31) Shuai, X.; He, Y.; Asakawa, N.; Inoue, Y. *J. Appl. Polym. Sci.* **2001**, *81*, 762−772.
(32) Zhang, L.; Goh, S. H.; Lee, S. Y. *Polymer* **1998**, *39*, 4841−4847.
(33) Coleman, M. M.; Serman, C. J.; Bhagwagar, D. E.; Painter, P. C. *Polymer* **1990**, *31*, 1187−1203.
(34) Zhang, L.; Goh, S. H.; Lee, S. Y. *J. Appl. Polym. Sci.* **1998**, *70*, 811−816.
(35) Nakahama, S.; Hirao, A. *Prog. Polym. Sci.* **1990**, *15*, 299.
(36) Arshady, R.; Kenner, G. W. *J. Polym. Sci., Part A: Polym. Chem.* **1974**, *12*, 2017−2025.
(37) Arichi, S.; Sakamoto, N.; Yoshida, M.; Himuro, S. *Polymer* **1986**, *27*, 1761−1767.
(38) Savitzky, A.; Golay, M. J. E. *Anal. Chem.* **1964**, *36*, 1627−1639.
(39) Steiner, J.; Termonia, Y.; Deltour, J. *Anal. Chem.* **1972**, *44*, 1906−1909.
(40) Edwards, T. H.; Willson, P. D. *Appl. Spectrosc.* **1974**, *28*, 541−545.
(41) Bank, M.; Leffingwell, J.; Thies, C. *Macromolecules* **1971**, *4*, 43.
(42) Kelts, L. W.; Landry, C. J. T.; Teegarden, D. M. *Macromolecules* **1993**, *26*, 2941.
(43) Couchman, P. R.; Karasz, F. E. *Macromolecules* **1978**, *11*, 1156.
(44) Kwei, T. K.; Pearce, J. R.; Pennacchia, J. R.; Charton, M. *Macromolecules* **1987**, *20*, 1174.
(45) Iriondo, P.; Iruin, J. J.; Fernandez-Berridi, M. J. *Macromolecules* **1996**, *29*, 5605−5610.
(46) Kuo, S. W.; Huang, C. F.; Chang, F. C. *J. Polym. Sci., Part B: Polym. Phys.* **2001**, *39*, 1348−1359.
(47) Kister, G.; Cassanas, G.; Vert, M. *Polymer* **1998**, *39*, 267−273.
(48) Cassanas, G.; Kister, G.; Fabrègue, E.; Morssli, M.; Bardet, L. *Spectrochim. Acta, Part A* **1993**, *49*, 271.
(49) Matsuura, H.; Yoshida, H.; Hieda, M.; Yamanaka, S.; Harada, T.; Fshin-ya, K.; Ohno, K. *J. Am. Chem. Soc.* **2003**, *125*, 13910−13911.
(50) Coleman, W. M.; Gordon, B. M. *Appl. Spectrosc.* **1987**, *41*, 1159−62.
(51) Coleman, W. M.; Gordon, B. M. *Appl. Spectrosc.* **1987**, *41*, 1163−9.
(52) Vaz, P. D.; Ribeiro-Claro, P. J. A. *J. Phys. Chem., Part A* **2003**, *107*, 6301−6305.
(53) Cataliotti, R.; Jones, R. N. *Spectrochim. Acta, Part A* **1971**, *27*, 2011.
(54) Mayo D. W.; Pike, R. M.; Butcher, S. S.; Trumper, P. K. *Microscale Techniques for the Organic Laboratory*; John Wiley and Sons, Inc.; New York, 1991.
(55) Bertran, J. F.; Ballester, L.; Dobrihalova, L.; Sánchez, N.; Arrieta, R. *Spectrochim. Acta, Part A* **1968**, *24*, 1765.
(56) Sato, H.; Murakami, R.; Padermshoke, A.; Hirose, F.; Senda, K. Noda, I. Ozaki, Y. *Macromolecules* **2004**, *37*, 7203−7213.
(57) Coleman, M. M.; Graf, J. F.; Painter, P. C. *Specific Interactions and the Miscibility of Polymer Blends*; Technomic Publishing, Inc.; Lancaster, PA, 1991.
(58) Flory, P. J. *Principles of Polymer Chemistry*; Cornell University Press: Ithaca, New York, 1953.
(59) Nishi, T.; Wang, T. T. *Macromolecules* **1975**, *8*, 915.
(60) Hoffman, J. D.; Weeks, J. J. *J. Res. Natl. Bur. Stand.* **1962**, *66*, 13.
(61) Fischer, E. W.; Stertzel, H. J.; Wegner, G. *Kolloid Z. Z. Polym.* **1973**, *251*, 980.
(62) Ziska, J. J.; Barlow, J. W.; Paul, D. R. *Polymer* **1981**, *22*, 918.
(63) Schindler, A.; Harper, D. H. *J. Polym. Sci., Polym. Chem. Ed.* **1979**, *17*, 2593.
(64) Skrovanek, D. J.; Howe, S. E.; Painter P. C.; Coleman, M. M. *Macromolecules* **1985**, *18*, 1676.
(65) Green, R. D. *Hydrogen bonding by C−H groups*; Wiley: New York, 1974.

MA047818F